



Article

# Extracellular Protein Aggregates Colocalization and Neuronal Dystrophy in Comorbid Alzheimer's and Creutzfeldt–Jakob Disease: A Micromorphological Pilot Study on 20 Brains

Nikol Jankovska <sup>1,\*</sup> , Tomas Olejar <sup>1</sup> and Radoslav Matej <sup>1,2,3</sup>

<sup>1</sup> Department of Pathology and Molecular Medicine, Third Faculty of Medicine, Charles University and Thomayer University Hospital, Videnska 800, 4-Krc, 14059 Prague, Czech Republic; tomas.olejar@ftn.cz (T.O.); radoslav.matej@ftn.cz (R.M.)

<sup>2</sup> Department of Pathology, First Faculty of Medicine, Charles University, and General University Hospital, 4-Krc, 14059 Prague, Czech Republic

<sup>3</sup> Department of Pathology, Third Faculty of Medicine, Charles University, and University Hospital Kralovske Vinohrady, 4-Krc, 14059 Prague, Czech Republic

\* Correspondence: nikol.jankovska@ftn.cz; Tel.: +420-261-083-102

**Abstract:** Alzheimer's disease (AD) and sporadic Creutzfeldt–Jakob disease (sCJD) are both characterized by extracellular pathologically conformed aggregates of amyloid proteins—amyloid  $\beta$ -protein ( $A\beta$ ) and prion protein ( $PrP^{Sc}$ ), respectively. To investigate the potential morphological colocalization of  $A\beta$  and  $PrP^{Sc}$  aggregates, we examined the hippocampal regions (archicortex and neocortex) of 20 subjects with confirmed comorbid AD and sCJD using neurohistopathological analyses, immunohistochemical methods, and confocal fluorescent microscopy. Our data showed that extracellular  $A\beta$  and  $PrP^{Sc}$  aggregates tended to be, in most cases, located separately, and “compound” plaques were relatively rare. We observed  $PrP^{Sc}$  plaque-like structures in the periphery of the non-compact parts of  $A\beta$  plaques, as well as in tau protein-positive dystrophic structures. The AD ABC score according to the NIA–Alzheimer's association guidelines, and prion protein subtype with codon 129 methionine–valine (M/V) polymorphisms in sCJD, while representing key characteristics of these diseases, did not correlate with the morphology of the  $A\beta/PrP^{Sc}$  co-aggregates. However, our data showed that  $PrP^{Sc}$  aggregation could dominate during co-aggregation with non-compact  $A\beta$  in the periphery of  $A\beta$  plaques.

**Keywords:** Creutzfeldt–Jakob disease; Alzheimer's disease;  $A\beta$ ; prion protein; tau protein; colocalization; plaques; confocal microscopy



**Citation:** Jankovska, N.; Olejar, T.; Matej, R. Extracellular Protein Aggregates Colocalization and Neuronal Dystrophy in Comorbid Alzheimer's and Creutzfeldt–Jakob Disease: A Micromorphological Pilot Study on 20 Brains. *Int. J. Mol. Sci.* **2021**, *22*, 2099. <https://doi.org/10.3390/ijms22042099>

Academic Editor: Mehdi Kabani

Received: 31 January 2021

Accepted: 17 February 2021

Published: 20 February 2021

**Publisher's Note:** MDPI stays neutral with regard to jurisdictional claims in published maps and institutional affiliations.



**Copyright:** © 2021 by the authors. Licensee MDPI, Basel, Switzerland. This article is an open access article distributed under the terms and conditions of the Creative Commons Attribution (CC BY) license (<https://creativecommons.org/licenses/by/4.0/>).

## 1. Introduction

Deposits of extracellular protein aggregates are diagnostic findings for two separate neurodegenerative diseases, i.e., Alzheimer's (AD) and Creutzfeldt–Jakob diseases (CJD) [1,2]. Amyloid- $\beta$  peptide ( $A\beta$ ) is a main defining component of  $A\beta$  plaques (also called amyloid or senile plaques) observed in AD [3,4]. These extracellular deposits arise from the amyloidogenic cleavage of an integral membrane protein, called amyloid precursor protein (APP), by beta-site APP cleaving enzyme 1 ( $\beta$ -secretase/BACE 1), which is found on neuronal membranes [5]. In addition to APP and BACE 1, the physiological isoform of the prion protein ( $PrP^C$ ) is also found on the outer surface of neuronal membranes; it is attached to the membrane via a glycosylphosphatidylinositol (GPI) anchor [6].

A full understanding of the physiological role of  $A\beta$  and  $PrP^C$  remains elusive. Briefly,  $A\beta$  plays a critical role in brain development, neuronal migration, and synaptic plasticity [7]. Additionally,  $A\beta$  interacts with Cu and Zn ions, e.g., rising copper levels increase the amount of APP on cell surfaces [8]; therefore, the increased presence of Cu ions mediates the precipitation of  $A\beta$  deposits [9]. Data from murine gene knock-outs suggest a functional

role for PrP<sup>C</sup> in myelination maintenance in adults, neuronal plasticity in adults, and the circadian rhythm [10].

Currently, molecular interactions between A $\beta$  and PrP, in either physiological or pathological forms, are being widely investigated, with interactions between oligomeric A $\beta$  and physiological PrP<sup>C</sup> receiving particular attention [11]. Other studies have focused on transfected SH-SY5Y neuroblastoma cells, cellular overexpression of PrP, decreased amyloidogenic cleavage of APP, and silencing of PrP<sup>C</sup> genes in N2A cells, via the increased secretion of A $\beta$  [12].

It has also been shown that the scrapie isoform of prion protein (PrP<sup>Sc</sup>) could alter APP processing through stimulation of 3-phosphoinositide-dependent protein kinase 1 (PDK1 or PDK2) and the inhibition of alpha-secretase activity, which could lead to enhanced  $\beta$ -secretase processing accompanied by increased A $\beta$  production [13]. There is another connection between these two proteins; as  $\gamma$ -secretase cleaves the residual APP C-terminal fragment, thus creating A $\beta$ , it leaves behind the amyloid intracellular domain (AICD) [14], which according to recent research, controls the expression of PrP<sup>C</sup> [15].

Membrane PrP<sup>C</sup> acts as a receptor for A $\beta$  oligomers; this feature helps explain its involvement in AD development [16]. Nonetheless, both AD and CJD have been described as having very similar dystrophic neurites containing mostly autophagic vacuoles and autophagosomes [17].

Even though microtubule-associated protein (MAP) tau mainly forms intracellular amyloid aggregates in AD, its functional interaction with PrP<sup>C</sup> and PrP<sup>Sc</sup> has also been reported. PrP<sup>C</sup> probably plays a critical role related to A $\beta$  and tau protein in AD development [18], with PrP<sup>C</sup> acting as a mediator of synaptic dysfunction induced by tau protein [19]. It is not unreasonable to expect dystrophic neurites with hyperphosphorylated tau protein in neuritic amyloid plaques. As such, dystrophic neurites in plaque-like PrP<sup>Sc</sup> structures that colocalize with A $\beta$  would also not be unexpected. There is increasing evidence that more than one neurodegeneration in the brain is possible at the same time [20]. However, the precise interactions among crucial amyloidogenic proteins in the pathophysiology of neurodegenerations remain unclear. Moreover, there is only limited information related to the morphological interactions among these brain peptides during comorbid neurodegenerations.

In our pilot study, we evaluated using immunohistochemistry and confocal microscopy, the micromorphology of PrP<sup>Sc</sup> colocalized with A $\beta$  in dystrophic neurites with compound plaques in the brains of patients with comorbid Alzheimer's and Creutzfeldt-Jakob disease [21].

## 2. Results

### 2.1. Confocal Microscopy Visualization

Using confocal fluorescent microscopy, we observed relatively rare compound plaques with either A $\beta$  or hyperphosphorylated tau protein (h-tau) in colocalization with PrP<sup>Sc</sup>. In co-aggregation with A $\beta$ , PrP<sup>Sc</sup> aggregates colocalized mainly with the non-compact (diffuse) regions of A $\beta$  plaques, while only minor colocalization was observed in the dense regions (see Figures 1 and 2). In contrast, no colocalization between h-tau and PrP<sup>Sc</sup> was observed, except for a few dot-like colocalizations (see Figure 3).

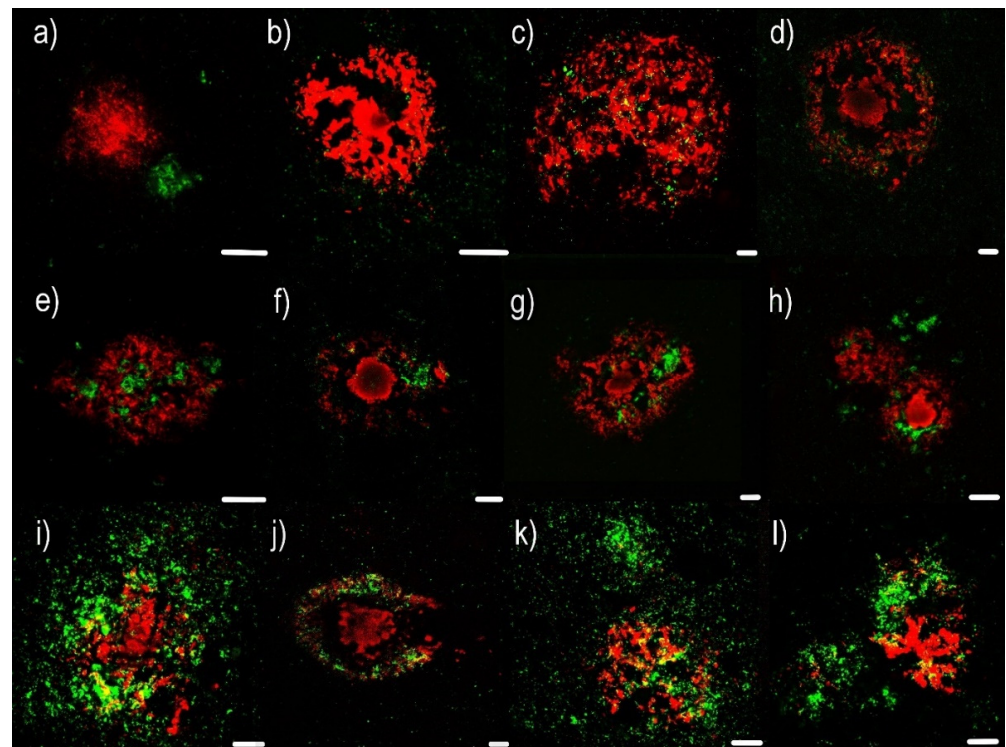


**Figure 1.** Immunofluorescence visualization of different types of anti-amyloid  $\beta$ -protein ( $A\beta$ ) and prion protein ( $PrP^{Sc}$ ) compound plaques in comorbid Alzheimer's (AD) and Creutzfeldt-Jakob diseases (CJD) cases. Primary antibodies: anti- $PrP$  (rabbit recombinant monoclonal antibody) + anti-amyloid  $\beta$ -protein (mouse monoclonal antibody). The secondary antibody was conjugated with either Alexa Fluor<sup>®</sup> 488 (anti-rabbit IgG; green) or Alexa Fluor<sup>®</sup> 568 (anti-mouse IgG; red). Scale bars indicate 10 micrometers. Images come from the hippocampal region (archicortical parts). (a,b) Non-compound plaques: consisting of (a)  $A\beta$  diffuse or (b) cored neuritic plaques, and lacking co-aggregating  $PrP$  structures. Images come from a 75-year-old female suffering from sCJD + AD (A1B1C1), cerebral amyloid angiopathy (CAA) 0. (c,d) Minimal compound plaques: diffuse (c) or cored neuritic (d)  $A\beta$  plaques with punctate  $PrP$  aggregates. Images come from a 69-year-old female suffering from sCJD + AD (A2B2C1), CAA 0. (e–h) Central core deposits: Neuritic non-cored (e) or cored (f–h)  $A\beta$  plaques with distinct  $PrP^{Sc}$  aggregates in the center of the plaque. Images come from two patients—a 79-year-old man suffering from sCJD + AD (A2B2C2), CAA 0, + ARTAG + Fahr disease, and a 71-year-old female sCJD + AD (A2B1C2), CAA. (i,j) Diffuse compound plaques: these are (i) neuritic non-cored or (j) cored  $A\beta$  plaques where co-aggregation of  $PrP^{Sc}$  at the periphery in the area of the non-compact  $A\beta$  structures is evident. The samples come from a 64-year-old male suffering from sCJD + early-onset AD (A2B2C2), CAA 0 + Wernicke's encephalopathy. (k,l) Diffuse "Yin-Yang" compound plaques: neuritic non-cored  $A\beta$  plaques having a prominent admixture of  $PrP^{Sc}$  co-aggregation predominantly localized at one pole of the plaque. The images come from a 70-year-old female patient sCJD + AD (A2B2C3) + CAA 0.

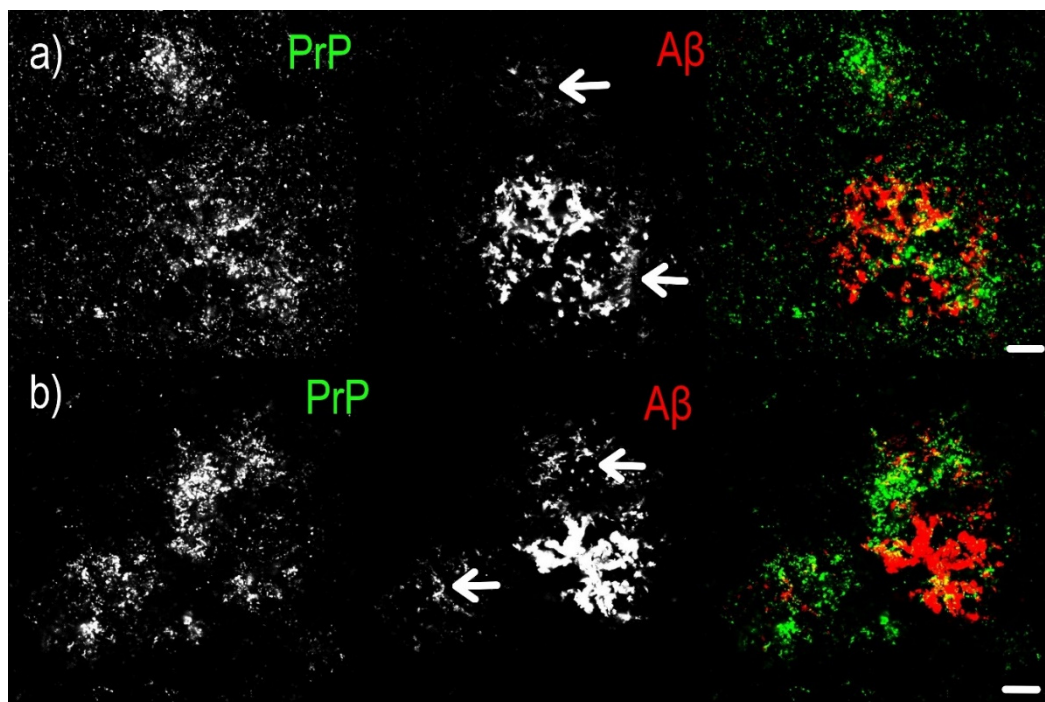


**Figure 2.** Immunofluorescence visualization and visualization of separated channels showing colocalization of PrP<sup>Sc</sup> with A $\beta$  in two different (a,b) non-cored plaques to demonstrate colocalization with more examples. PrP<sup>Sc</sup> aggregates colocalized predominantly with non-compact A $\beta$  of the senile plaques, while only a minor colocalization was observed in the dense parts. Both images (a,b) show diffuse “Yin-Yang” compound plaques. Arrows point to non-compact areas of A $\beta$  plaques. Scale bars indicate 10 micrometers.

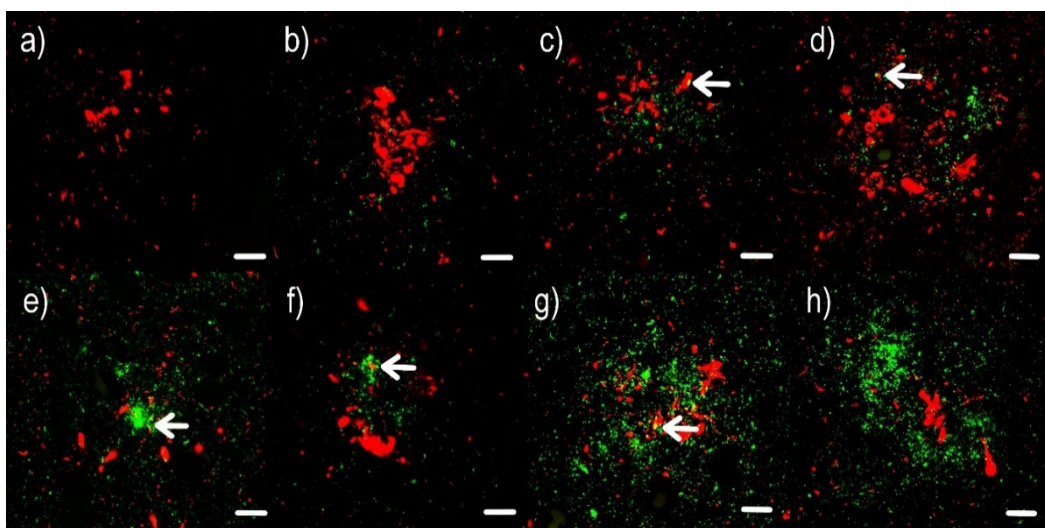


**Figure 3.** Immunofluorescence visualization of h-tau-positive dystrophic neurites in colocalization with PrP<sup>Sc</sup> aggregates in comorbid AD and CJD cases (a–h). Primary antibodies: PrP (rabbit recombinant monoclonal antibody) + AT8 (mouse monoclonal antibody). The secondary antibody was conjugated with either Alexa Fluor<sup>®</sup> 488 (anti-rabbit IgG, green) or Alexa Fluor<sup>®</sup> 568 (anti-mouse IgG, red). Scale bars indicate 10 micrometers. Arrows indicate minor colocalization of AT8 with PrP. Images come from the hippocampal region (archicortical parts).

Visualization of comorbid CJD and AD cases revealed that plaques varied with regard to the micromorphologies of A $\beta$  with PrP<sup>Sc</sup> between patients. In all subjects, one particular type of A $\beta$  and PrP<sup>Sc</sup> colocalization predominated. The main types of A $\beta$  and PrP<sup>Sc</sup> plaque colocalizations identified were (Figure 1):

- (1) Non-compound and minimal compound plaques (10 cases out of 17):
  - a. Non-compound plaques (observed in 3 cases out of 17) are without co-occurrence or colocalization of A $\beta$  and PrP<sup>Sc</sup> deposits. Pure A $\beta$  and pure PrP<sup>Sc</sup> plaque exist independently of each other (Figure 1a,b).
  - b. Minimal compound plaques (Figure 1c,d) were seen most often (7 of 17 patients in whom PrP<sup>Sc</sup> aggregates were present in the neocortical and archicortical parts of the hippocampal region). The most prominent feature of minimal compound plaques was A $\beta$  (in the form of non-cored or cored plaque); however, dotted PrP<sup>Sc</sup>-immunoreactivities were also present.
- (2) Central core deposits—this pattern occurred in both non-cored and cored A $\beta$  plaques (3 cases out of 17). In these cases, a rather significant PrP<sup>Sc</sup> positivity was observed in central non-compact A $\beta$  plaque structures, either with or without dense A $\beta$  cores (Figure 1e–h).
- (3) Diffuse plaques (4 cases out of 17):
  - a. Diffuse compound plaques (Figure 1i,j) contain PrP<sup>Sc</sup> diffusely scattered in the periphery of condensed A $\beta$  plaques and are colocalized with surrounding non-compact A $\beta$  (seen in a single case).
  - b. Diffuse so-called “Yin Yang” compound plaques (Figure 1k,l; Figure 2) are a particular subset of asymmetric diffuse compound plaques in which PrP<sup>Sc</sup>-positive structures are polarized to the sides of asymmetric plaques in colocalization with non-compact A $\beta$  periphery (i.e., non-compact A $\beta$  in colocalization with PrP<sup>Sc</sup>, but not surrounding the entire circumference of the compact A $\beta$  core aggregates). This type of plaques was observed in 3 cases out of 17.

Similar to colocalization with A $\beta$  in plaques, minimal dot-like colocalization with h-tau positive dystrophic neurites in plaques was recorded (Figure 3).

We analyzed the density and type of colocalization relative to the biochemical and neuropathological properties of CJD and AD; however, no association between plaque micromorphology, type of colocalization, polymorphism at codon 129, type of PrP<sup>Sc</sup>, and the AD ABC score according to the NIA-Alzheimer’s association guidelines was observed (Charts 1–3).

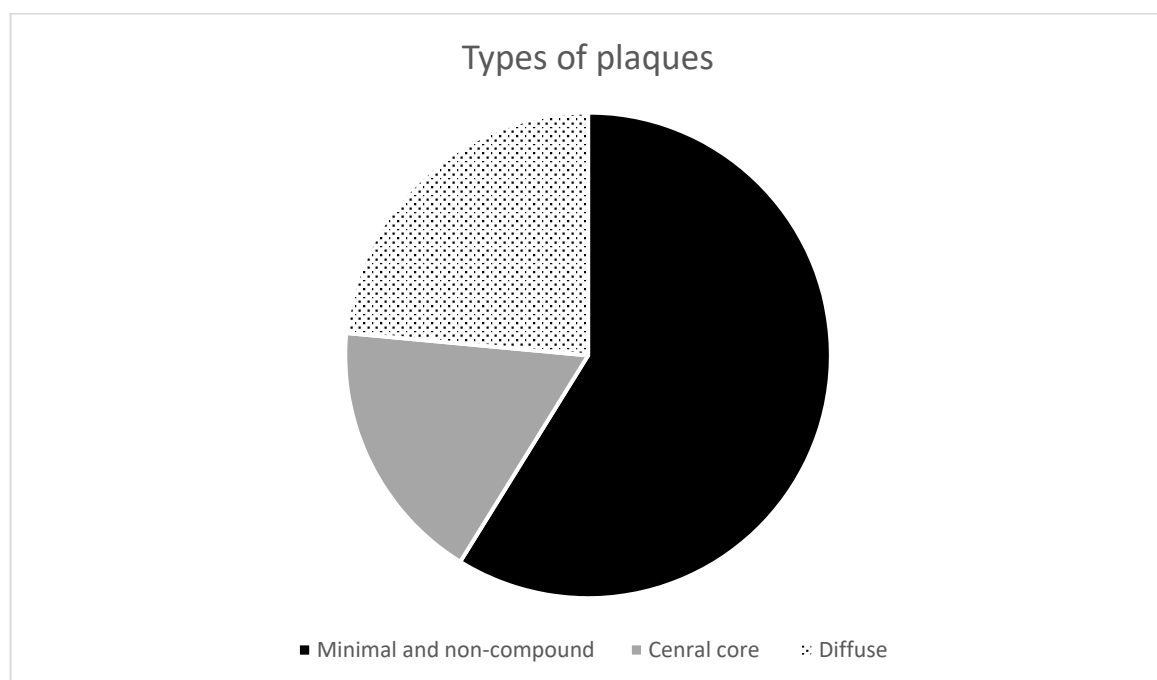


**Chart 1.** Relative rate of individual types of A $\beta$  and PrP<sup>Sc</sup> colocalization in plaque.

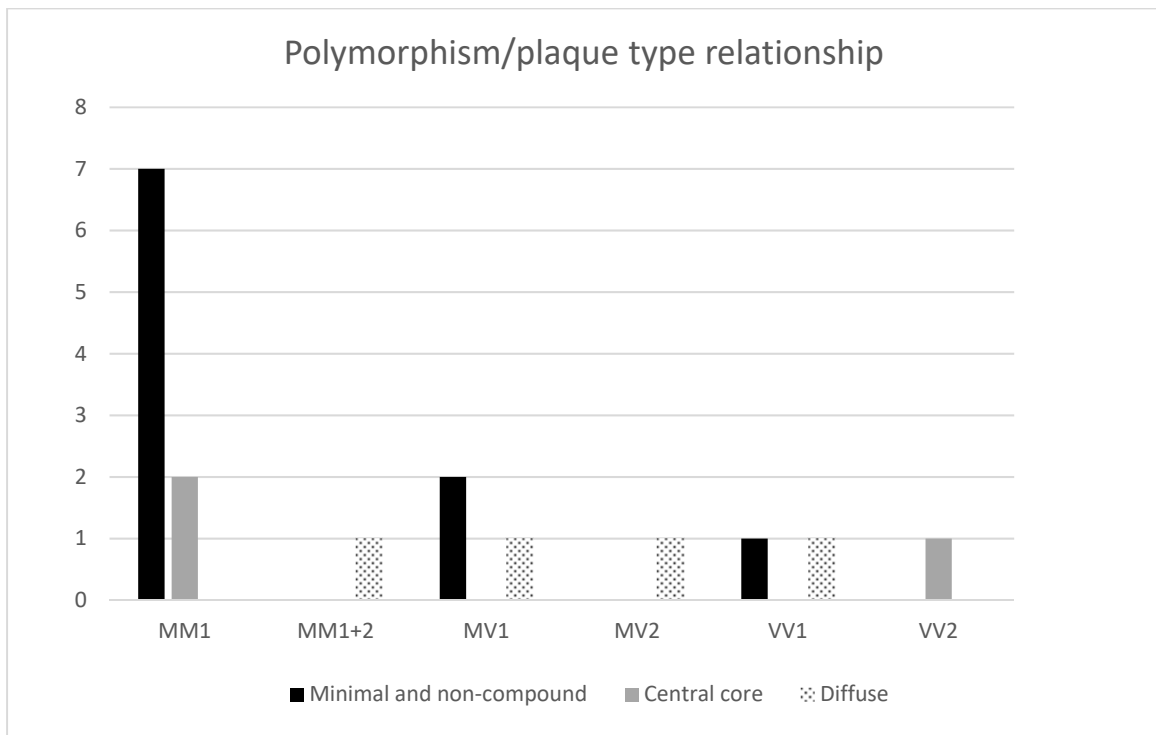


**Chart 2.** Relationship between methionine–valine (M/V) polymorphisms and plaque type.

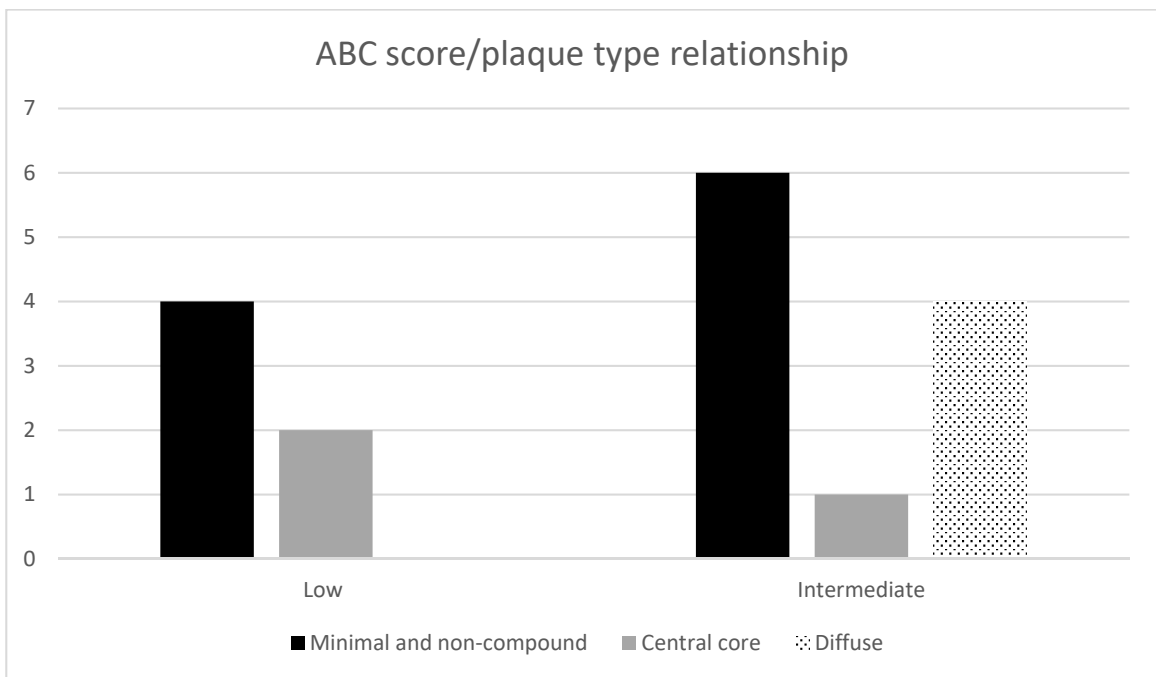


**Chart 3.** Dependence of plaque-type on the ABC scores.

### 2.2. Immunohistochemical Examination

In the immunohistochemical examination, parallel imaging of PrP, hyperphosphorylated tau protein (AT8), and A $\beta$  aggregates in the same hippocampal area (Figure 4a,c) clearly showed the occurrence of PrP<sup>Sc</sup>-positive aggregates in plaques with h-tau positive dystrophic neurites where A $\beta$  was entirely missing. Thus, this observation also suggests

that PrP<sup>Sc</sup> could be colocalized with h-tau-positive dystrophic neurites in A $\beta$  plaques in the absence of A $\beta$  structures.

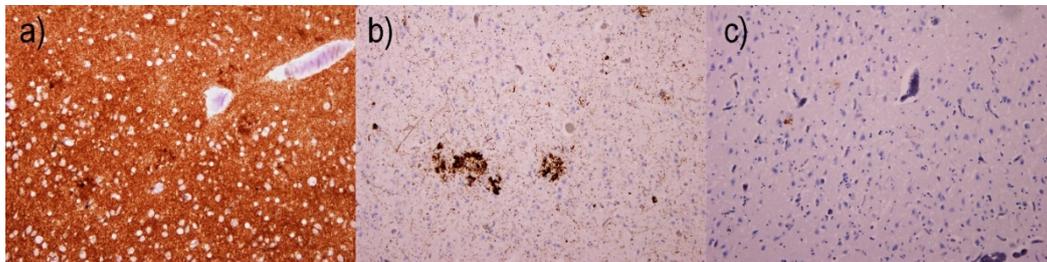


**Figure 4.** Immunohistochemical imaging of (a) PrP<sup>Sc</sup>-positive plaque-like structures, (b) AT8-positive dystrophic neurites, and (c) A $\beta$  plaques in the same hippocampal region (archicortical part) of an 80-year-old female patient. There are PrP<sup>Sc</sup> “plaque-like” deposits and h-tau positive neuritic plaques in the same area lacking the equivalent of A $\beta$  plaques. The secondary antibody was conjugated with horseradish peroxidase staining DAB. The original magnification is 100 $\times$ .

### 3. Discussion

In the study presented, a particular affinity of PrP<sup>Sc</sup> for the non-compact parts of A $\beta$  plaques, suggesting that different subspecies of A $\beta$  have different affinities for PrP<sup>Sc</sup> aggregates, was observed. In addition, previously reported low rate of compound plaques colocalizing with A $\beta$  or h-tau and PrP<sup>Sc</sup> in comorbid AD and sCJD were considered.

The potential interaction between PrP<sup>Sc</sup> and A $\beta$  in comorbid AD and sCJD remains controversial. No significant correlation has been reported for variables influencing the development of CJD and variables determining the course of AD [22]. On the other hand, colocalization of PrP<sup>Sc</sup> and A $\beta$  in single plaques was reported in a patient with a rare prion disease called Gerstmann–Sträussler–Scheinker disease (GSS) [23]; however, this colocalization was only observed in GSS and not in sCJD [24]. On the contrary, other authors reported compound PrP<sup>Sc</sup> and A $\beta$  plaques in 11 of 12 evaluated subjects with a concomitant sCJD and AD pathology; the frequency of compound plaques ranged between 2 and 29% [25]. Others also documented the presence of PrP<sup>C</sup> in senile plaques in non-sCJD AD describing dot-like PrP<sup>C</sup>-immunoreactivity in diffuse plaques, isolated large coarse PrP<sup>C</sup>-positive structures in neuritic plaques, and dense non-compact or amorphous aggregates in amyloid cores of senile plaques [26].

As mentioned above, the colocalization of A $\beta$  and PrP<sup>Sc</sup> in different prionopathies in comorbidity with AD was reported, and the frequency of these compound plaques was demonstrated. On the contrary, this study was focused on the detailed micromorphological relationship of PrP<sup>Sc</sup>, A $\beta$ , and AT8 in compound plaques based on confocal fluorescent microscopy.

Based on this, we recognized three types of A $\beta$  and PrP<sup>Sc</sup> colocalization, as follows: (1) no or minimum compound plaques, (2) compound plaques with a centrally dense PrP<sup>Sc</sup> core only, and (3) compound plaques with or without a centrally dense PrP<sup>Sc</sup> core; however, PrP<sup>Sc</sup> was always present in the periphery. Our data show no or minimal colocalization in the compact region of A $\beta$  plaques; however, in the non-compact region of A $\beta$  plaques, which were often located in the periphery, showed a higher rate of colocalization. Non-compact A $\beta$  plaques are mostly composed of A $\beta$ <sub>42</sub>, rather than A $\beta$ <sub>40</sub> [27]. Similar to a study on single and double immunohistochemical stains of PrP<sup>C</sup> in A $\beta$  plaques in AD patients [26], we observed an abundance of dot-like aggregates in diffuse plaques, while in neuritic plaques, PrP deposits tended to be relatively coarse. Interestingly, there seems to be no association between plaque micromorphology, polymorphism at codon 129, type of PrP<sup>Sc</sup>, and the AD ABC scores.

In addition, AT8 positive dystrophic neurites were observed in colocalization with PrP<sup>Sc</sup> plaque-like structures. Dystrophic; dilated; and, in specific locations, bulbous dystrophic neurites are a common feature of A $\beta$  plaques [21] in AD. Thus, it is not surprising

that these structures, which were detected by immunohistochemical positivity of hyperphosphorylated tau protein, are also observed in colocalization with PrP<sup>Sc</sup>. However, using simple DAB immunohistochemistry, we were able to find hippocampal regions with PrP<sup>Sc</sup> plaque-like positivity and h-tau-positive A $\beta$  plaques without the expression of A $\beta$  (Figure 4), suggesting that direct interaction between PrP<sup>Sc</sup> and dystrophic neurites or directly with h-tau. Direct molecular interactions between PrP<sup>Sc</sup> and tau protein have also been reported [28]. Conversely, tau pathology presented as neurofibrillary tangles was a pathognomonic finding for the Indiana Kindred variant of GSS [29]. In the P105L variant of GSS, dystrophic, tau-positive neurites and neurofibrillary tangles were observed in PrP<sup>Sc</sup> plaques, even in the absence of senile A $\beta$  amyloid plaques [30]. Associations between PrP<sup>Sc</sup> plaques and tau aggregation were observed in scrapie-infected mouse brains of human tau transgenic mice [31]. Thus, direct pathological interactions between PrP<sup>Sc</sup> and tau in the absence of A $\beta$  facilitating the progression of the disease could be a plausible hypothesis for AD and sCJD comorbidity. However, our observations are based on a pilot study with a small cohort of patients, and lack a control group with separate AD and CJD cohorts. The results are sustainable for further investigation.

#### 4. Materials and Methods

##### 4.1. Patients

A total of 20 patients diagnosed with comorbid AD and CJD (age range 62–83 years, median age 71 years) were neuropathologically defined using the National Institute on Aging Alzheimer’s Association (NIA-AA) consensus scheme [32]. Additionally, the presence of PrP<sup>Sc</sup> in brain tissue was confirmed by both Western-blot and immunohistochemistry. The patient characteristics are summarized in Table 1, which includes gender, age, disease duration, the AD ABC score, [33] codon 129 methionine and/or valine polymorphisms, PrP<sup>Sc</sup> [34] isoform (i.e., type 1 or 2), specification of other vascular and age-related co-pathologies, and the presence of protein 14-3-3 in the cerebrospinal fluid.

**Table 1.** Individual patients, including gender, age, duration of the disease, 129 codon polymorphisms with the PrP type, 14-3-3 positivity, the AD ABC score according to the NIA-Alzheimer’s association guidelines, data regarding other neuropathologies, and plaque type specification.

No.	Sex	Age	Duration (Months)	Polymorph.	PrP Types Brain Tissue	Western Blot (14-3-3) CSF	AD ABC Score	Other Neuropathology	Type of Plaques
1.	M	75	2	MM	1	neg.	A2B2C2	Angiosclerotic encephalopathy, ARTAG, encephalomalacia	Non-compound
2.	F	71	1	MV	1	low pos.	A2B1C2	Angiosclerotic encephalopathy	Non-compound
3.	F	75	9	VV	1	pos.	A1B1C1	Angiosclerotic encephalopathy	Non-compound
4.	F	67	1	MM	1	pos.	A2B1C1	Angiosclerotic encephalopathy	Minimal compound
5.	F	69	2	MM	1	NA	A2B2C1	Angiosclerotic encephalopathy	Minimal compound
6.	M	62	6	MV	1	neg.	A3B2C2	Angiosclerotic encephalopathy	Minimal compound
7.	F	65	2	MM	1	pos.	A2B2C2	Angiosclerotic encephalopathy	Minimal compound
8.	M	79	1	MM	1	pos.	A1B2C1	Angiosclerotic encephalopathy	Minimal compound
9.	M	75	4	MM	1	neg.	A2B2C2	Angiosclerotic encephalopathy, ARTAG, Wernicke encephalopathy, meningioma	Minimal compound
10.	F	68	2	MM	1	pos.	A2B2C2	Angiosclerotic encephalopathy, AGD	Minimal compound + few compounds
11.	M	79	1,5	MM	1	pos.	A2B2C2	Angiosclerotic encephalopathy, ARTAG	Central core deposits

Table 1. Cont.

No.	Sex	Age	Duration (Months)	Polymorph.	PrP Types Brain Tissue	Western Blot (14-3-3) CSF	AD ABC Score	Other Neuropathology	Type of Plaques
12.	F	71	1	MM	1	pos.	A2B1C2	Angiosclerotic encephalopathy	Central core deposits
13.	F	80	2	VV	2	pos.	A3B1C2	Angiosclerotic encephalopathy	Central core deposits
14.	M	64	2	MV	2	low pos.	A2B2C2	Angiosclerotic encephalopathy, Wernicke encephalopathy	Diffuse compound
15.	F	70	2	VV	1	pos.	A2B2C2	Angiosclerotic encephalopathy	Yin-Yang
16.	F	70	1	MM	1 + 2	pos.	A2B2C3	Angiosclerotic encephalopathy	Yin-Yang
17.	F	80	5	MV	1	pos.	A3B2C3	Angiosclerotic encephalopathy	Yin-Yang + few compounds
18.	M	83	1	MM	1	low pos.	A2B2C2	Angiosclerotic encephalopathy, ARTAG	Lacking PrP plaques in the hippocampus
19.	F	65	5	VV	1	pos.	A1B1C1	Angiosclerotic encephalopathy	Lacking PrP plaques in the hippocampus
20.	M	85	2	MM	1	neg.	A2B2C2	Angiosclerotic encephalopathy	Lacking PrP plaques in the hippocampus

M—male; F—female; MM/MV/VV—methionine and/or valine polymorphism on codon 129; CSF—cerebrospinal fluid; ARTAG—aging-related tau astroglialopathy; AGD—argyrophilic grain disease; PrP—prion protein.

All data were analyzed with respect to patient privacy, and the study was conducted in accordance with the Ethics Committee of Thomayer University Hospital (No G-19-18) on 10 April 2019.

#### 4.2. Tissue Samples

Brain tissue samples were fixed for 3–4 weeks in buffered 10% formalin. Then, selected tissue blocks, using a standardized protocol BrainNet Europe [35], were embedded in paraffin using an automatic tissue processor. Five- $\mu$ m-thick sections were prepared and stained with hematoxylin–eosin, Klüver–Barrera, and silver impregnation methods. For analysis, representative blocks of the left hippocampal and parahippocampal areas were chosen.

#### 4.3. Immunofluorescence and Immunohistochemistry

Briefly, 5- $\mu$ m-thick sections of formalin-fixed and paraffin-embedded tissue samples were deparaffinized and then incubated with primary antibodies for 20 min at room temperature. For A $\beta$  and PrP<sup>Sc</sup> antibody staining, 96% formic acid was applied prior to the primary antibody. A second layer for light microscopy visualization, consisting of secondary horseradish peroxidase-conjugated antibody (En Vision FLEX/HRP, Dako M822, Glostrup, Denmark), was applied for 20 min at room temperature. The samples were then incubated with DAB (Substrate—Chromogen Solution, Dako K3468, Glostrup, Denmark) for 10 min to visualize the reaction. Mayer's Hematoxylin Solution was used as a counterstain.

For confocal microscopy, secondary antibodies conjugated to Alexa Fluor® (see below) were used. Paraffin sections were also treated with 20X TrueBlack® (Biotium 23007, Fremont, CA, USA) diluted in 1X 70% alcohol to quench lipofuscin autofluorescence.

##### 4.3.1. Primary Antibodies

For immunohistochemistry, 5- $\mu$ m-thick sections of formalin-fixed and paraffin-embedded tissue were selected from the hippocampal region, including the entorhinal and transentorhinal cortex. These were incubated with primary antibodies against the following

antigens: (1) A $\beta$  (1:1000, mouse monoclonal, clone 6F/3D; Dako M0872, Glostrup, Denmark), (2) A $\beta$  (1:5000, rabbit monoclonal, clone H31L21; Thermo Fisher Scientific 700254, Waltham, ME, USA), (3) PrP (1:8000, mouse monoclonal, clone 12F10; Bertin Pharma A03221, Bordeaux, France), (4) PrP (1:3000, mouse monoclonal, clone 6H8; Prionics 7500996, Schlieren, CH), (5) PrP (1:5000, rabbit recombinant monoclonal, clone SC57-05; Thermo Fisher Scientific MA5-32202, Waltham, ME, USA), and (6) Phospho-Tau (Ser202, Thr205) Monoclonal Antibody (1:500, mouse monoclonal, clone AT8; Thermo Fisher Scientific MN1020, Waltham, ME, USA).

#### 4.3.2. Secondary Antibodies

Detection of immunostaining was carried out using horseradish peroxidase–diaminobenzidine (see above) for immunohistochemistry and secondary antibodies conjugated with Alexa Fluor<sup>®</sup> 488 (1:1000, donkey anti-rabbit, H + L IgG, Thermo Fisher Scientific, Waltham, MA, USA) and Alexa Fluor<sup>®</sup> 568 (1:1000, donkey anti-mouse, H + L IgG, Thermo Fisher Scientific) for immunofluorescence staining. Slides incubated with only the secondary antibody were used as specificity controls.

#### 4.4. Microscopy Evaluation

##### 4.4.1. Light Microscopy

The samples were examined independently by two neuropathologists focused predominantly on the archicortical parts of hippocampal region, and the presence/absence of A $\beta$  deposits and AT8-positive structures, in relation to PrP deposits, was evaluated. An Olympus BX51 microscope (Olympus Europa SE and Co. KG, Hamburg, Germany) was used for examination with 100 $\times$  magnification. Images were captured with an Olympus DP72 camera controlled using Olympus image analysis software (Olympus Europa SE and Co. KG).

##### 4.4.2. Confocal Microscopy

Colocalization of pathogenic protein aggregates was imaged using a Leica TCS SP5 confocal fluorescent laser scanning microscope (Leica Microsystems Inc., Wetzlar, Germany). The HCX PL APO objective with 40 $\times$  magnification, oil immersion, and a pinhole of 1 AU was used. Donkey anti-Rabbit IgG secondary antibody was conjugated to Alexa Fluor<sup>®</sup> 488 and excited at 488 nm using a 65 mW multi-line argon laser, whereas Donkey anti-Mouse IgG conjugated to Alexa Fluor<sup>®</sup> 568 was excited at 561 nm using a 20 mW DPSS laser.

##### 4.4.3. Classification of A $\beta$ Plaques

Diffuse, neuritic non-cored and neuritic cored A $\beta$  plaques were classified according to the literature, as previously summarized in a review article [20].

## 5. Conclusions

The results as presented indicate that a specific subset of A $\beta$ , in particular the non-compact component of A $\beta$  plaque where A $\beta$ <sub>42</sub> predominates, exhibits higher levels of interaction with PrP<sup>Sc</sup> and, thus, in certain circumstances, could be assumed to act as the PrP<sup>Sc</sup> seeds within the brain (see Supplementary Materials). The role of PrP<sup>Sc</sup> in the development of neuritic plaques, with or without the A $\beta$  component, certainly requires further investigation.

**Supplementary Materials:** The following are available online at <https://www.mdpi.com/1422-0067/22/4/2099/s1>.

**Author Contributions:** The authors confirm contribution to the paper as follows: study conception and design: R.M., T.O.; data collection: N.J.; analysis and interpretation of results: N.J., T.O., R.M.; draft manuscript preparation: N.J. All authors have read and agreed to the published version of the manuscript.

**Funding:** This study was supported by the Ministry of Health, Czech Republic (Conceptual development of research organization VFN64165); the General University Hospital, Prague; the Thomayer Hospital, Prague (TN64190); the Grants Agency of the Ministry of Health (NV19-04-00090 and NV18-04-00179); and by Charles University (Project Progress Q27/LF1 and GAUK 142120).

**Institutional Review Board Statement:** The study was conducted according to the guidelines of the Declaration of Helsinki approved in advance by the Ethics Committee of the Institute for Clinical and Experimental Medicine and Thomayer University Hospital for the Research Project entitled: “Simultaneous histology imaging of neurodegenerative comorbidities utilizing fluorescent and multichannel confocal microscopy” on 10 April 2019.

**Informed Consent Statement:** No informed consent obtained as only archival tissue of dead subjects was investigated retrospectively in anonymous setting with respect to their privacy, no treatment or diagnostic intervention was performed.

**Data Availability Statement:** The authors confirm that all data underlying the findings are fully available without restriction. All data are included within the manuscript <https://doi.org/10.3390/ijms22042099>.

**Acknowledgments:** The authors wish to thank Tom Secest, MSc, for the revision of the English version of this article.

**Conflicts of Interest:** The authors declare no conflict of interest.

## References

1. Huang, W.-J.; Chen, W.-W.; Zhang, X. Prions mediated neurodegenerative disorders. *Eur. Rev. Med. Pharmacol. Sci.* **2015**, *19*, 4028–4034.
2. Thal, D.R.; Walter, J.; Saito, T.C.; Fändrich, M. Neuropathology and biochemistry of A $\beta$  and its aggregates in Alzheimer’s disease. *Acta Neuropathol.* **2015**, *129*, 167–182. [[CrossRef](#)]
3. Obeng, R. Amyloid Beta and Amyloid Beta Precursor Protein. Available online: <https://www.pathologyoutlines.com/topic/stainsamyloidbetaapp.html> (accessed on 12 November 2020).
4. Litak, J.; Mazurek, M.; Kulesza, B.; Szmygin, P.; Litak, J.; Kamieniak, P.; Grochowski, C. Cerebral Small Vessel Disease. *Int. J. Mol. Sci.* **2020**, *21*, 9729. [[CrossRef](#)]
5. Ben Halima, S.; Mishra, S.; Raja, K.M.P.; Willem, M.; Baici, A.; Simons, K.; Brüstle, O.; Koch, P.; Haass, C.; Caflisch, A.; et al. Specific Inhibition of  $\beta$ -Secretase Processing of the Alzheimer Disease Amyloid Precursor Protein. *Cell Rep.* **2016**, *14*, 2127–2141. [[CrossRef](#)]
6. Singh, J.; Udgaonkar, J.B. Molecular Mechanism of the Misfolding and Oligomerization of the Prion Protein: Current Understanding and Its Implications. *Biochemistry* **2015**, *54*, 4431–4442. [[CrossRef](#)]
7. Van Der Kant, R.; Goldstein, L.S. Cellular Functions of the Amyloid Precursor Protein from Development to Dementia. *Dev. Cell* **2015**, *32*, 502–515. [[CrossRef](#)] [[PubMed](#)]
8. Gamez, P.; Caballero, A.B. Copper in Alzheimer’s disease: Implications in amyloid aggregation and neurotoxicity. *AIP Adv.* **2015**, *5*, 092503. [[CrossRef](#)]
9. Atwood, C.S.; Scarpa, R.C.; Huang, X.; Moir, R.D.; Jones, W.D.; Fairlie, D.P.; Tanzi, R.E.; Bush, A.I. Characterization of Copper Interactions with Alzheimer Amyloid  $\beta$  Peptides. *J. Neurochem.* **2008**, *75*, 1219–1233. [[CrossRef](#)]
10. Watts, J.C.; Bourkas, M.E.C.; Arshad, H. The function of the cellular prion protein in health and disease. *Acta Neuropathol.* **2017**, *135*, 159–178. [[CrossRef](#)] [[PubMed](#)]
11. Gunther, E.C.; Strittmatter, S.M.  $\beta$ -amyloid oligomers and cellular prion protein in Alzheimer’s disease. *J. Mol. Med.* **2010**, *88*, 331–338. [[CrossRef](#)]
12. Parkin, E.T.; Watt, N.T.; Hussain, I.; Eckman, E.A.; Eckman, C.B.; Manson, J.C.; Baybutt, H.N.; Turner, A.J.; Hooper, N.M. Cellular prion protein regulates beta-secretase cleavage of the Alzheimer’s amyloid precursor protein. *Proc. Natl. Acad. Sci. USA* **2007**, *104*, 11062–11067. [[CrossRef](#)]
13. Ezpeleta, J.; Baudouin, V.; Arellano-Anaya, Z.E.; Boudet-Devaud, F.; Pietri, M.; Baudry, A.; Haeberlé, A.-M.; Bailly, Y.; Kellermann, O.; Launay, J.-M.; et al. Production of seedable Amyloid- $\beta$  peptides in model of prion diseases upon PrP<sup>Sc</sup>-induced PDK1 overactivation. *Nat. Commun.* **2019**, *10*, 1–13. [[CrossRef](#)] [[PubMed](#)]
14. Plant, L.D.; Boyle, J.P.; Smith, I.F.; Peers, C.; Pearson, H.A. The Production of Amyloid  $\beta$  Peptide Is a Critical Requirement for the Viability of Central Neurons. *J. Neurosci.* **2003**, *23*, 5531–5535. [[CrossRef](#)] [[PubMed](#)]
15. Vincent, B.; Sunyach, C.; Orzechowski, H.-D.; George-Hyslop, P.S.; Checler, F. p53-Dependent Transcriptional Control of Cellular Prion by Presenilins. *J. Neurosci.* **2009**, *29*, 6752–6760. [[CrossRef](#)]
16. Zhang, Y.; Zhao, Y.; Zhang, L.; Yu, W.; Wang, Y.; Chang, W. Cellular Prion Protein as a Receptor of Toxic Amyloid- $\beta$ 42 Oligomers Is Important for Alzheimer’s Disease. *Front. Cell. Neurosci.* **2019**, *13*, 339. [[CrossRef](#)]

17. Liberski, P.P. Axonal changes in experimental prion diseases recapitulate those following constriction of postganglionic branches of the superior cervical ganglion: A comparison 40 years later. *Prion* **2019**, *13*, 83–93. [CrossRef]
18. Gomes, L.A.; Hipp, S.A.; Upadhaya, A.R.; Balakrishnan, K.; Ospitalieri, S.; Koper, M.J.; Largo-Barrientos, P.; Uytterhoeven, V.; Reichwald, J.; Rabe, S.; et al. A $\beta$ -induced acceleration of Alzheimer-related  $\tau$ -pathology spreading and its association with prion protein. *Acta Neuropathol.* **2019**, *138*, 913–941. [CrossRef]
19. Ondrejčák, T.; Klyubin, I.; Corbett, G.T.; Fraser, G.; Hong, W.; Mably, A.J.; Gardener, M.; Hammersley, J.; Perkinson, M.S.; Billinton, A.; et al. Cellular Prion Protein Mediates the Disruption of Hippocampal Synaptic Plasticity by Soluble Tau In Vivo. *J. Neurosci.* **2018**, *38*, 10595–10606. [CrossRef] [PubMed]
20. Jankovska, N.; Olejar, T.; Matej, R. Extracellular Amyloid Deposits in Alzheimer's and Creutzfeldt–Jakob Disease: Similar Behavior of Different Proteins? *Int. J. Mol. Sci.* **2020**, *22*, 7. [CrossRef] [PubMed]
21. Jankovska, N.; Olejar, T.; Kukal, J.; Matej, R. Different Morphology of Neuritic Plaques in the Archicortex of Alzheimer's Disease with Comorbid Synucleinopathy: A Pilot Study. *Curr. Alzheimer Res.* **2021**, *17*, 948–958. [CrossRef] [PubMed]
22. Rossi, M.; Kai, H.; Baiardi, S.; Bartoletti-Stella, A.; Carlà, B.; Zenesini, C.; Capellari, S.; Kitamoto, T.; Parchi, P. The characterization of AD/PART co-pathology in CJD suggests independent pathogenic mechanisms and no cross-seeding between misfolded A $\beta$  and prion proteins. *Acta Neuropathol. Commun.* **2019**, *7*, 53. [CrossRef]
23. Furukawa, F.; Sanjo, N.; Kobayashi, A.; Hamaguchi, T.; Yamada, M.; Kitamoto, T.; Mizusawa, H.; Yokota, T. Specific amyloid- $\beta$ 42 deposition in the brain of a Gerstmann–Sträussler–Scheinker disease patient with a P105L mutation on the prion protein gene. *Prion* **2018**, *12*, 315–319. [CrossRef]
24. Miyazono, M.; Kitamoto, T.; Iwaki, T.; Tateishi, J. Colocalization of prion protein and beta protein in the same amyloid plaques in patients with Gerstmann–Sträussler Syndrome. *Acta Neuropathol.* **1992**, *83*, 333–339. [CrossRef]
25. Hainfellner, J.A.; Wanschitz, J.; Jellinger, K.; Liberski, P.P.; Gullotta, F.; Budka, H. Coexistence of Alzheimer-type neuropathology in Creutzfeldt–Jakob disease. *Acta Neuropathol.* **1998**, *96*, 116–122. [CrossRef]
26. Ferrer, I.; Blanco, R.; Carmona, M.; Puig, B.; Ribera, R.; Rey, M.J.; Ribalta, T. Prion protein expression in senile plaques in Alzheimer's disease. *Acta Neuropathol.* **2001**, *101*, 49–56. [CrossRef]
27. Duyckaerts, C.; Dickson, D.W. *Neurodegeneration: The Molecular Pathology of Dementia and Movement Disorders*, 2nd ed.; Wiley-Blackwell: Hoboken, NJ, USA, 2011; pp. 62–68. ISBN 978140519632.
28. Han, J.; Zhang, J.; Yao, H.; Wang, X.; Li, F.; Chen, L.; Gao, C.; Gao, J.; Nie, K.; Zhou, W.; et al. Study on interaction between microtubule associated protein tau and prion protein. *Sci. China Ser. C Life Sci.* **2006**, *49*, 473–479. [CrossRef]
29. Dlouhy, S.R.; Hsiao, K.; Farlow, M.R.; Foroud, T.; Conneally, P.M.; Johnson, P.; Prusiner, S.B.; Hodes, M.E.; Ghetti, B. Linkage of the Indiana kindred of Gerstmann–Sträussler–Scheinker disease to the prion protein gene. *Nat. Genet.* **1992**, *1*, 64–67. [CrossRef]
30. Ishizawa, K.; Mitsufuji, T.; Shioda, K.; Kobayashi, A.; Komori, T.; Nakazato, Y.; Kitamoto, T.; Araki, N.; Yamamoto, T.; Sasaki, A. An autopsy report of three kindred in a Gerstmann–Sträussler–Scheinker disease P105L family with a special reference to prion protein, tau, and beta-amyloid. *Brain Behav.* **2018**, *8*, e01117. [CrossRef]
31. Race, B.; Phillips, K.; Kraus, A.; Chesebro, B. Phosphorylated human tau associates with mouse prion protein amyloid in scrapie-infected mice but does not increase progression of clinical disease. *Prion* **2016**, *10*, 319–330. [CrossRef]
32. Montine, T.J.; Phelps, C.H.; Beach, T.G.; Bigio, E.H.; Cairns, N.J.; Dickson, D.W.; Duyckaerts, C.; Frosch, M.P.; Masliah, E.; Mirra, S.S.; et al. National Institute on Aging–Alzheimer's Association guidelines for the neuropathologic assessment of Alzheimer's disease: A practical approach. *Acta Neuropathol.* **2011**, *123*, 1–11. [CrossRef]
33. Hyman, B.T.; Phelps, C.H.; Beach, T.G.; Bigio, E.H.; Cairns, N.J.; Carrillo, M.C.; Dickson, D.W.; Duyckaerts, C.; Frosch, M.P.; Masliah, E.; et al. National Institute on Aging–Alzheimer's Association guidelines for the neuropathologic assessment of Alzheimer's disease. *Alzheimer Dement.* **2012**, *8*, 1–13. [CrossRef]
34. Parchi, P.; De Boni, L.; Saverioni, D.; Cohen, M.L.; Ferrer, I.; Gambetti, P.; Gelpi, E.; Giaccone, G.; Hauw, J.-J.; Höftberger, R.; et al. Consensus classification of human prion disease histotypes allows reliable identification of molecular subtypes: An inter-rater study among surveillance centres in Europe and USA. *Acta Neuropathol.* **2012**, *124*, 517–529. [CrossRef]
35. Autopsy. Netherlands Brain Bank. Available online: <https://www.brainbank.nl/brain-tissue/autopsy/> (accessed on 14 February 2021).